https://doi.org/10.5194/acp-2022-548
Preprint. Discussion started: 12 August 2022

Atmospheric Chemistry and Physics Discussions

Elucidate the Formation Mechanism of Particulate Nitrate Based on Direct Radical Observations in Yangtze River Delta summer 2019

Tianyu Zhai[a], *Keding Lu*[a, b*], *Haichao Wang*[c], *Shengrong Lou*[d], *Xiaorui Chen*[a, f], *Renzhi Hu*[e], *Yuanhang Zhang*[a, b*]

[a] State Key Joint Laboratory of Environmental Simulation and Pollution Control, College of Environmental Sciences and Engineering, Peking University, Beijing 100871, China.

[b] Collaborative Innovation Center of Atmospheric Environment and Equipment Technology, Nanjing University of Information Science & Technology, Nanjing 210044, China.

[c] School of Atmospheric Sciences, Sun Yat-sen University, Guangzhou 510275, China.

[d] State Environmental Protection Key Laboratory of Formation and Prevention of the Urban Air Complex, Shanghai Academy of Environmental Sciences, Shanghai, 200223, China.

[e] Key Laboratory of Environmental Optics and Technology, Anhui Institute of Optics and Fine Mechanics, Chinese Academy of Sciences, Hefei, 230031, China.

[f] Now at: Department of Civil and Environmental Engineering, The Hong Kong Polytechnic University, Hong Kong, China.

[*] *Correspondence to:*

Keding Lu (k.lu@pku.edu.cn), Yuanhang Zhang (yhzhang@pku.edu.cn)

https://doi.org/10.5194/acp-2022-548
Preprint. Discussion started: 12 August 2022

Atmospheric Chemistry and Physics Discussions

Abstract. Particulate nitrate (NO_3^-) is the one of the dominant components of fine particles in China, especially during pollution episodes, and has a significant impact on human health, air quality and climate. Here a comprehensive field campaign which focus on the atmospheric oxidation capacity and aerosol formation, and their effects in Yangtze River Delta (YRD) had been conducted from May to June, 2019 at a regional site in Changzhou, Jiangsu province in China. The concentration of NO_3^-, OH radical, N_2O_5, NO_2, O_3 and relevant parameters were measured simultaneously. We showed a high NO_3^- mass concentration with 10.6 ± 8.9 μg m^{-3} on average, which accounted for 38.3 % of water-soluble components and 32.0 % total $PM_{2.5}$, and followed by the proportion of sulfate, ammonium and chloride by 26.0 %, 18.0 % and 2.0 %, respectively. This result confirmed the heavy nitrate pollution in eastern China not only happened in winter but also summer time. High nitrate oxidation ratio (NOR) during this study emphasizes the strong atmospheric oxidation and fast nitrate formation capacity in YRD. It is found that OH + NO_2 at daytime dominates nitrate formation on clean days while N_2O_5 hydrolysis largely enhanced and become comparable with that of OH + NO_2 during polluted days (47.1 % and 52.9 %). An updated observed-constrain Empirical Kinetic Modeling Approach (EKMA) was used to assess the kinetic controlling factors of both local O_3 and NO_3^- productions, which indicated that O_3-targeted scheme ($VOCs:NO_x$ = 2:1) is effective to mitigate the O_3 and nitrate pollution coordinately during summertime in this region. Our results promote the understanding of nitrate pollution mechanisms and mitigation based on field observation and model simulation, and call for more attentions to nitrate pollutions in summertime.

Keywords:
Nitrate pollution; Dinitrogen pentoxide; Nitrate formation; Pollution mitigation

1 Introduction

Chemical compositions of fine particle have been measured in China during past twenty

https://doi.org/10.5194/acp-2022-548
Preprint. Discussion started: 12 August 2022

Atmospheric Chemistry and Physics Discussions

years and secondary inorganic aerosol is regarded as one of the dominant species in aerosol (Cao et al., 2012; Hagler et al., 2006; Zhao et al., 2013; Andreae et al., 2008). Since the Air Pollution Prevention and Control Action Plan, there has been a significant decrease of SO_2, NO_2 and $PM_{2.5}$ concentration in China, while the inorganic nitrate ratio in $PM_{2.5}$ increased and became the considerable component in $PM_{2.5}$ (Shang et al., 2021; Zhang et al., 2022). Therefore, the comprehensive understanding of particlate nitrate foramtion mechanism is essential and critical to mitigate haze pollution in China.

A massive research have been taken in China for investigating nitrate formation mechanism and basic framework has been established (Sun et al., 2006; Chang et al., 2018; Wu et al., 2019). In daytime, NO_2 + OH radical oxidation (Reaction 1) is the major particulate nitrate formation pathway. The product (HNO_3) reacts with alkaline substance in aerosol by which generating particulate nitrate. This pathway mainly controled by precurors concentration as well as gas-particle partition of gaseous nitric acid and particulate nitrate depends on temperature, relative humidity (RH), NH_3 concentration and aerosol acidity (Wang et al., 2009; Song and Carmichael, 2001; Meng et al., 2020; Zhang et al., 2021). At night, N_2O_5 uptake is an important nitrate formation pathway (Reaction 4)(Chen et al., 2020; Wang et al., 2022). N_2O_5 is formed through NO_2 + NO_3 (Reaction 3) and there exsits a quick thermal equilibrium balance ($K_{eq} = 5.5 \times 10^{-17}$ cm^{-3} $molecule^{-1}$ s^{-1}, 298 K). However, there are two problems remain ambiguous in quantifying the contribution of N_2O_5 uptake to nitrate formation. The first is the N_2O_5 heterogeneous uptake coefficent (γ) on ambient aerosol is highly varied with the range from 10^{-4} to 10^{-1} based on previous lab and field measurments (Bertram and Thornton, 2009; Brown et al., 2009; Wang et al., 2017c; Wang and Lu, 2016). The other one is $ClNO_2$ production yield which inflences nitrate contribution duo to the large variation range (Phillips et al., 2016; Staudt et al., 2019; Tham et al., 2018). Both the two parameters are hardly to well-predicted by current schemes. Besides, N_2O_5 homogeneous hydrolysis, NO_2 heterogeneous uptake and NO_3 radical oxidation have minor contribution to particulate nitrate under ambient condition (Brown et al., 2009;

https://doi.org/10.5194/acp-2022-548
Preprint. Discussion started: 12 August 2022

Atmospheric Chemistry and Physics Discussions

Seinfeld and Pandis, 2016).

$$NO_2 + OH \rightarrow HNO_3 \quad \text{R1}$$

$$NO_2 + O_3 \rightarrow NO_3 + O_2 \quad \text{R2}$$

$$NO_2 + NO_3 + M \rightarrow N_2O_5 + M \quad \text{R3.1}$$

$$N_2O_5 + M \rightarrow NO_2 + NO_3 + M \quad \text{R3.2}$$

$$N_2O_5 + (H_2O \text{ or } Cl^-) \rightarrow (2 - \varphi)\, NO_3^- + \varphi ClNO_2 \quad \text{R4}$$

As a key area of China's economy and industry, Yangtze River Delta (YRD) has suffered severe air pollution during past decades and fine particle pollution in YRD has raised a widespread concern (Guo et al., 2014; Zhang et al., 2015; Zhang et al., 2017; Ming et al., 2017; Xue et al., 2019). However, most of these research focus on wintertime $PM_{2.5}$ pollution and lack of measurements of critical intermediate species and radicals to assess the importance of each nitrate formation pathway. In this study, with the direct measurements of hydroxyl radical and the reactive nitrogen compounds and chemical box model analysis, we explore the characteristics of nitrate and precursors in YRD in the summer of 2019, the importance of particulate nitrate formation pathways is quantified, and the impact factors are explored. Further suggestion for summer pollution prevention and control for local area is proposed.

2 Site description and methods

2.1 The campaign site

This campaign had been taken place at a sub-urban sanatorium from May 30th to June 18th 2019 at Changzhou, China. Changzhou (119.95 °E, 31.79 °N) is located at Jiangsu province and about 150 km northwest of Shanghai. The sanatorium which is located at 420 m east of Lake Ge (one of the largest lakes in Jiangsu province, 164 square kilometers) is surrounded by farmland and fishpond. With the closest arterial traffic 1 km away, there are several industry zones 4 km to the east. The prevailing wind was

https://doi.org/10.5194/acp-2022-548
Preprint. Discussion started: 12 August 2022

Atmospheric Chemistry and Physics Discussions

from south and south east sectors (about 30 % of the time) compared to 20 % from the west sector, of which only 15 % came from the east. The wind speed was normally lower than 5 m s^{-1} with faster speed from the west. This site was influenced by both anthropogenic and biological sources with occasionally biomass burning.

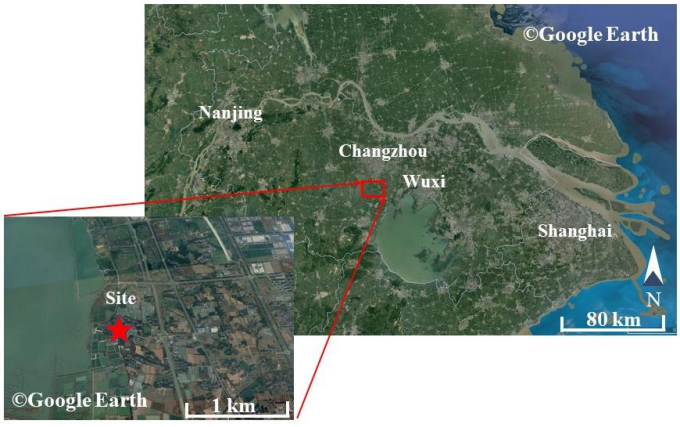

Figure 1 The location of campaign site (red star), Changzhou is located 150 km at the northwest side of Shanghai.

2.2 The instrumentation

To comprehensive interpret the nocturnal atmospheric capacity and aerosol formation, multiple gas and particle parameters were measured simultaneously and the related instruments are listed in Table 1. N_2O_5 and Particle Number and Size Distribution (PNSD) were measured on fourth floor of the sanatorium which is the top of the building. Other instruments were set up in containers placed on the ground and 170 m northeast of the building. These instruments monitored through the roof of containers and inlets were circa 5 m above the ground.

N_2O_5 was measured by Cavity Enhanced Absorption Spectrometer (CEAS) based on Lambert-Beer's law which was developed by (Wang et al., 2017b). Briefly, air samples were drawn through the window and reached out of the wall 30 cm to prevent influence from surface deposition. Aerosol membrane filter was deployed before

https://doi.org/10.5194/acp-2022-548
Preprint. Discussion started: 12 August 2022


Atmospheric Chemistry and Physics Discussions

sample PFA tube and changed every 2 hours during the night to avoid a decrease in N_2O_5 transmission efficiency due to the increased loss of N_2O_5 from the accumulated aerosols on the filter. N_2O_5 was decomposed to NO_3 and NO_2 through preheating tube which is heat at 130 ℃ and detected within a PFA-coated resonator cavity which is heated at 110 ℃ to prevent the formation of N_2O_5 by reversible reaction subsequently. At the end of each sampling cycle (5 min), 30 s injection of high concentration NO (10 ppm, 20 ml min^{-1}) which mixed with sample air was set to eliminate NO_3-N_2O_5 in the system. The NO titration spectrums were adopted as dynamic background spectrum by assuming that no H_2O concentration variation in single sampling cycle. The loss of N_2O_5 in the sampling system and filter were considered within data correction. The limit of detection (LOD) was estimated to be 2.7 pptv (1 σ) with an uncertainty of 19 %.

OH radical measurement was conducted by Fluorescence Assay by Gas Expansion Laser-Induced Fluorescence techniques (FAGE-LIF), ambient air was expanded through a 0.4 mm nozzle to low pressure in a detection chamber, in where OH radical irradiated by the 308 nm laser pulse at a repetition rate of 8.5 kHz (Chen et al., 2018). NO_x and O_3 were monitored by commercial monitors (Thermo-Fisher 42i and 49i). Volatile organic compounds (VOCs) were measured by using automated Gas Chromatograph equipped with a Mass Spectrometer and flame ionization detector (GC-MS) with a time resolution of 60 min. The photolysis frequencies were determined from the spectral actinic photon flux density measured by spectroradiometer (Bohn et al., 2008).

$PM_{2.5}$ concentration was obtained by Tapered Element Oscillating Microbalance (TEOM 1405, Thermo Scientific Inc). Aerosol surface concentration (S_a) was converted from particle number and size distribution which measured by Scanning Mobility Particle Sizer (SMPS, TSI 3936) and Aerosol Particle Sizer (APS, TSI 3321) and modified to the wet particle-state S_a with a hygroscopic growth factor (Liu et al., 2013). The uncertainty of the wet S_a was ~ 30 %. Meanwhile, water-soluble particulate species as well as their gaseous precursors were analyzed through the Monitor for

https://doi.org/10.5194/acp-2022-548
Preprint. Discussion started: 12 August 2022

Atmospheric Chemistry and Physics Discussions

AeRosols and GAses in ambient air (MARGA, Chen et al. (2017)). Meteorological data, including the temperature, relative humidity (RH), pressure, wind speed, and wind direction, were also available.

Table 1 The observed gas and particle parameters during the campaign.

Parameters	Detection of limit	Method	Accuracy
N_2O_5	2.7 pptv (1 σ, 1 min)	CEAS	± 19 %
OH	1.6×10^5 cm^{-3} (1 σ, 60 s)	LIF[a]	± 21 %
NO	60 pptv (2 σ, 1 min)	PC[c]	± 10 %
NO_2	0.3 ppbv (2 σ, 1 min)	PC[c]	± 10 %
O_3	0.5 ppbv (2 σ, 1 min)	UV photometry	± 5 %
VOCs	20-300 pptv (60 min)	GC-MS	± 15 %
$PM_{2.5}$	0.1 μg m^{-3} (1 min)	TEOM[d]	± 5 %
Photolysis frequencies	5×10^{-5} s^{-1} (1 min)	SR[e]	± 10 %
PNSD	14 nm -700 nm (4 min)	SMPS, APS	± 10 %
HNO_3, NO_3, HCl	0.06 ppbv (30 min)	MARGA[f]	± 20 %
NH_4^+, NO_3^-, Cl^-, SO_4^{2-}	0.05 μg m^{-3} (30 min)	MARGA[f]	± 20 %

[a] Laser-induced fluorescence; [b] Chemiluminescence; [c] Photolytic converter; [d] Tapered Element Oscillating Microbalance; [e] Spectroradiometer; [f] the Monitor for AeRosols and GAses in ambient air.

2.3 The empirical kinetic modelling approach

A box-model coupled with the Regional Atmospheric Chemical Mechanism version 2 (RACM2, Goliff, Stockwell & Lawson, 2013) is used to conduct the mitigation strategies studies. The model is operated in one-hour time resolution with measurement results of temperature, relative humidity, pressure, CO, NO_2, H_2O, photolysis frequencies and aggregated VOCs input to constrain the model. It should be noted that HONO concentration is simply calculated by NO_2 times 0.02 which is suggested by Elshorbany et al. (2012) and has been used in box model before (Lou et al., 2022). Long-live species such as H_2 and CH_4 are set as constants (550 ppbv and 1900 ppbv respectively). What's more, a 13-hour constant loss rate of unconstrained intermediate and secondary products, which is the result of synthetic evaluating secondary simulation of secondary species, is set for representing the multi-effects of deposition, transformation and transportation.

The approaches of chemical production of O_3 ($P(O_3)$) and inorganic nitrate

https://doi.org/10.5194/acp-2022-548
Preprint. Discussion started: 12 August 2022

Atmospheric Chemistry and Physics Discussions

(P(NO_3^-)) are using previously described expression (Tan et al., 2021; Tan et al., 2018) in Equation 1 and 4:

$$P(O_3) = F(O_3) - D(O_3) \quad \text{Eq1}$$

$$F(O_3) = k_{HO_2+NO}[NO][HO_2] + k_{(RO_2+NO)eff}[NO][RO_2] \quad \text{Eq2}$$

$$D(O_3) = k_{OH+NO_2}[OH][NO_2] + (k_{OH+O_3}[OH] + k_{HO_2+O_3}[HO_2] + k_{alkenes+O_3}[alkenes])[O_3] \quad \text{Eq3}$$

$$P(NO_3^-) = P(HNO_3) + P(pNO_3^-) \quad \text{Eq4}$$

$$P(HNO_3) = k_{OH+NO_2}[OH][NO_2] \quad \text{Eq5}$$

$$P(pNO_3^-) = 0.25(2 - \varphi)\, C\, \gamma\, S_a\, [N_2O_5] \quad \text{Eq6}$$

briefly, $P(O_3)$ is net ozone production which calculated by peroxyl radial + NO oxidation (Eq. 2) minus chemical loss of O_3 and NO_2 (Eq. 3). $P(NO_3^-)$ is constituted by reaction OH + NO_2 (Eq. 5) and N_2O_5 heterogenous uptake (Eq. 6). Here, rate constants of reactions are obtained from NASA JPL Publication (Burkholder et al., 2015) or RACM2 (Goliff et al., 2013). γ is the N_2O_5 uptake coefficient which is calculated from parameterization (γ_P, more details in chapter 3.3). φ represents $ClNO_2$ production yield through N_2O_5 hydrolysis and the mean value reported in Xia et al. (2020) are used in this work.

Empirical Kinetic Modeling Approach (EKMA) was innovated for studying the effects of precursors VOCs, NOx reactivity on the region's ozone pollution by Kanaya et al, which help recognize the region's susceptibility to precursors by weight and become a prevalent tool to study the process of ozone formation (Tan et al., 2018; Yu et al., 2020b; Kanaya et al., 2008). The prevention and control problem of pollutant generation can be transformed through EKMA curve to reduce its precursors emissions. Furthermore, the precursors reduction scheme needed for pollutant total control is given qualitatively. $P(NO_3^-)$ can also be analyzed through EKMA for the nonlinear secondary formation relationship with precursor reactivity. Here, isopleth diagram of the net ozone production rate as functions of the reactivities of NO_x and VOCs can be derived from EKMA. In detail, 0.01 to 1.2 emission reduction strategy assumptions are exponential interpolation into 20 kinds of emission situation of NO_x and VOCs respectively, which in total counts 400 scenarios.

2.4 The calculation of aerosol liquid water content

Aerosol liquid water content (ALWC) is calculated through ISORROPIA II

https://doi.org/10.5194/acp-2022-548
Preprint. Discussion started: 12 August 2022


Atmospheric Chemistry and Physics Discussions

(Fountoukis and Nenes, 2007). Forward mode is applied in this study. Furthermore, water-soluble ions in $PM_{2.5}$ and gaseous species (NH_3 + HNO_3 + HCl) obtained from MARGA, along with RH and T are input as initial input. In addition, metastable aerosol state is chosen since high RH during this campaign.

3 Result and discussion

3.1 Overview of measurements

The time used in this study is China Standard Time (UTC + 8) and the local sunrise and sunset time during the campaign were around 5 am and 7 pm, respectively. The whole campaign period is divided into the four $PM_{2.5}$ clean periods and four $PM_{2.5}$ polluted periods (9 out of 14 days, latter polluted periods and day refer to $PM_{2.5}$ pollution except specified description) according to the Chinese National Air Quality Standard (CNAAQS) Grade I of daily $PM_{2.5}$ concentrations (< 35.0 μg m^{-3}). Figure 2 shows the meteorological parameters, gas-phase and particulate species timeseries during the observation. During the campaign, the temperature was high and the maximum reached 34.5 ℃, with an average 25.1 ± 3.7 ℃. RH changed drastically from 21 % to 88 %, with mean value at 58.9 ± 14.0 %. Mean NO_2 concentration was 14.8 ± 9.5 ppbv. Meanwhile, O_3 average was 54.6 ± 28.8 ppbv, exceeding CNAAQS Grade II for maximum daily average 8 h ozone (160 μg m^{-3}) on 14 out of 19 days and exceeding 200 μg m^{-3} on 6 days.

https://doi.org/10.5194/acp-2022-548
Preprint. Discussion started: 12 August 2022

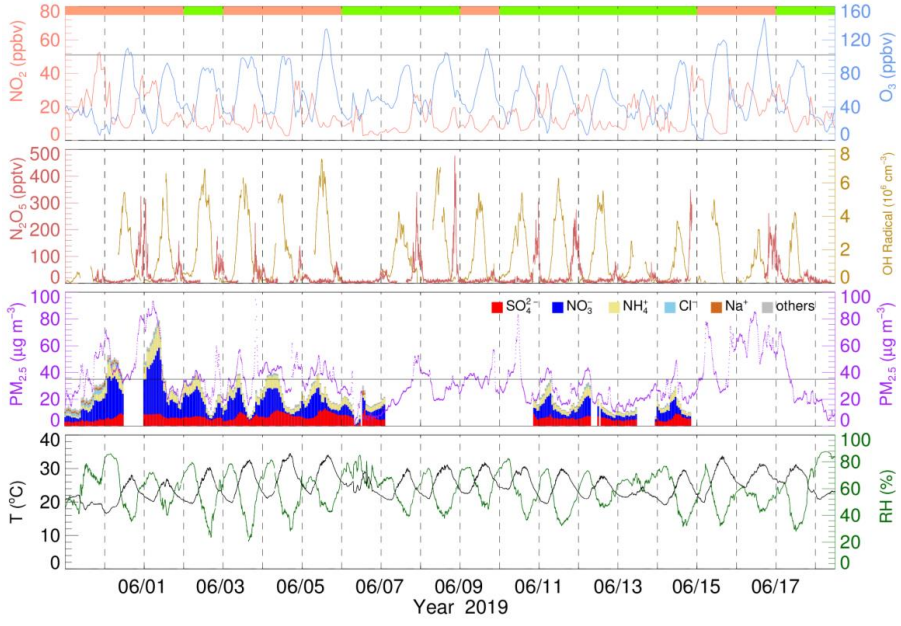

Figure 2 Timeseries of NO_2, O_3, N_2O_5, OH radical, $PM_{2.5}$ and water-soluble particulate species, temperature and RH. The vertical dotted line represents zero clock. The black horizontal solid line in O_3 and $PM_{2.5}$ panel represents Chinese national air quality standard for O_3 and $PM_{2.5}$ respectively. Top panel color blocks represent $PM_{2.5}$ clean day (light green) and $PM_{2.5}$ polluted day(salmon) respectively.

Daytime OH radical ranged from 2×10^6 to 8×10^6 molecular cm^{-3} with daily peak over 3×10^6 molecular cm^{-3}. Maximum OH radical reached 8.18×10^6 molecular cm^{-3} in this campaign. Comparing with other summertime OH radical observed campaign in China, OH radical concentration in this site is relatively low but still on the same order of magnitude (Lu et al., 2012; Lu et al., 2013; Ma et al., 2022; Tan et al., 2017; Woodward-Massey et al., 2020; Yang et al., 2021). N_2O_5 mean concentration was 21.9 ± 39.8 pptv with nocturnal average 61.0 ± 63.1 pptv and daily maximum over 200 pptv at 8 nights. The maximum concentration of N_2O_5 (477.2 pptv, 5 min resolution) appeared at 20:47 June 8th. The average NO_3 radical production rate $P(NO_3)$ is 2.1 ± 1.4 ppbv h^{-1} with nocturnal average $P(NO_3)$ 2.8 ± 1.6 ppbv h^{-1} and daytime $P(NO_3)$ 2.2 ± 1.4 ppbv h^{-1}. $P(NO_3)$ is about twice of documented value in Taizhou and North China Plain (Wang et al., 2017a; Wang et al., 2018b; Wang et al., 2020a), but close to another

https://doi.org/10.5194/acp-2022-548
Preprint. Discussion started: 12 August 2022

Atmospheric Chemistry and Physics Discussions

result in YRD before (Chen et al., 2019). Average of $PM_{2.5}$ was 34.6 ± 17.8 μg m^{-3} with maximum reach 163.0 μg m^{-3}. The water-soluble components of $PM_{2.5}$ are displayed as well, the average NO_3^- concentration was 10.6 μg m^{-3}, which accounts for 38.3 % mass concentration of water-soluble components and 32.0 % total $PM_{2.5}$, while proportion of sulfate, ammonium and chloride are 26.0 %, 18 % and 2.0 % respectively. To sum up, during campaign period, the pollution of $PM_{2.5}$ would be exacerbated in general on high O_3 and NO_2 days. Precipitation occurred during four clean processes receded pollutant concentration, otherwise, the pollution condition remained severe.

The mean diurnal variations (MDC) of temperature, RH, NO_2, O_3, $P(NO_3)$, N_2O_5, OH radical and $PM_{2.5}$ in different air quality are shown in Figure 3. The temperature, RH and OH radical MDC show indistinctive difference between clean day (CD) and polluted day (PD). The MDC of NO_2 has two concentration peaks appeal at 06:00 and 21:00 on CD, while at PD, its peak appeals at 20:00 and maintain high level during whole night. O_3 diurnal pattern reflects a typical urban-influenced character with maximum O_3 peak lasts four hours from 14:00 to 17:00 with polluted-day O_3 peak concentration 1.2 higher than clean-day. $P(NO_3)$ grows after O_3 peak and maximum $P(NO_3)$ shows at 19:00 with average value 1.7 ppbv h^{-1} on clean day. By contrast, mean polluted-day $P(NO_3)$ is 2.6 ppbv h^{-1} and maximum value reach 4.7 ppbv h^{-1}. In contrast, the clean-day N_2O_5 has higher average and maximum concentration than PD which suggests faster removal process during PD. $PM_{2.5}$ have similar trend with $P(NO_3)$ and has higher concentration during nighttime.

https://doi.org/10.5194/acp-2022-548
Preprint. Discussion started: 12 August 2022

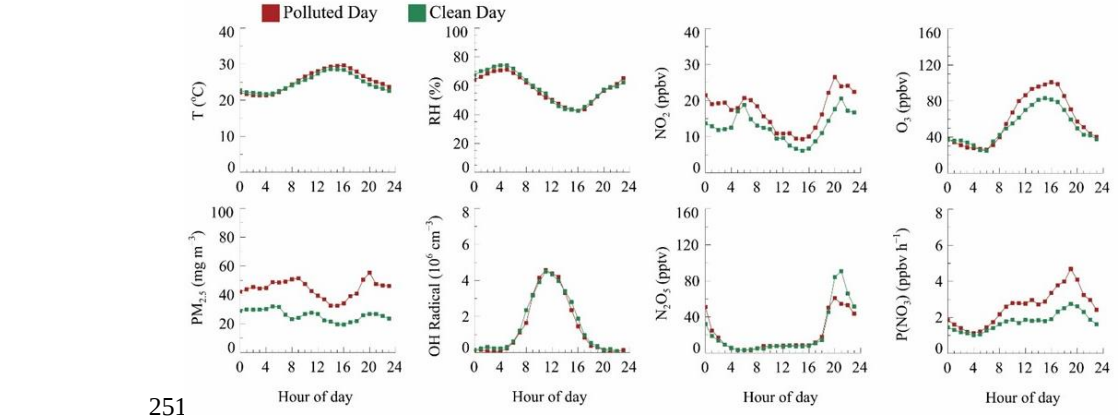

Figure 3 The mean diurnal variations of temperature, RH, NO_2 (Salmon), O_3, $P(NO_3)$, N_2O_5, OH radical(orange) and $PM_{2.5}$ of clean day and polluted day.

3.2 The evolution of nitrate pollution

Figure 4 (a) shows the relationship of nitrate and sulfate with water-soluble ion. Nitrate has positive correlation with particulate water-soluble ion while sulfate ratio having inverse correlation. With $PM_{2.5}$ concentration increasing, nitrate proportion increasing rapidly and keep high weight at heavy $PM_{2.5}$ period while sulfate appears opposite phenomenon. Once the mass concentration of water-soluble ion over 30 μg m^{-3}, the mass fraction of nitrate in total water-soluble ion is up to 50 % on average. This result illustrates that particulate nitrate is one of the vital sources of particulate matter explosive growth.

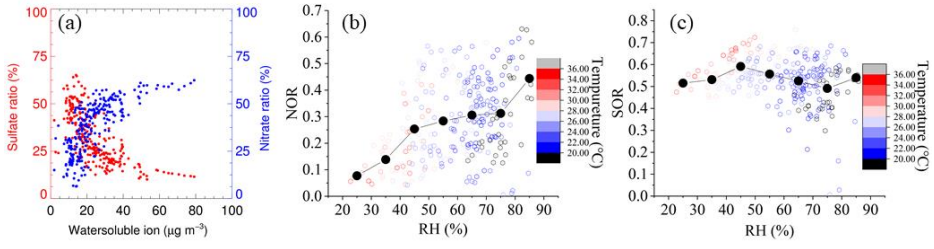

Figure 4 (a) Particulate ion mass concentration ratio of nitrate and sulfate to water soluble ion. (b) NOR against RH, colored with temperature. (c) SOR against RH, colored with temperature.

https://doi.org/10.5194/acp-2022-548
Preprint. Discussion started: 12 August 2022

Atmospheric Chemistry and Physics Discussions

To further assess the conversion capacity of nitrate and sulfate in this site, the sulfur oxidation ratio (SOR) and the nitrogen oxidation ratio (NOR) are used for indicating secondary transformation ratio of SO_2 and NO_2 respectively (Sun et al., 2006). SOR and NOR are estimated using formulae below:

$$SOR = \frac{nSO_4^{2-}}{nSO_4^{2-}+nSO_2} \quad \text{Eq7}$$

$$NOR = \frac{nNO_3^-}{nNO_3^-+nNO_2} \quad \text{Eq8}$$

here n refers to the molar concentration. The higher SOR and NOR represent more oxidation of gaseous species into secondary aerosol. As depicted in Figure 4 (b-c), NOR rapid increases at RH < 45 %, remains constant at 45 % < RH < 75 % and ends with a sharply increase at RH > 75 %. In addition, NOR has inverse correlation with temperature which reflects the importance of nighttime secondary transformation and the influence of negative correlation of gas-solid equilibrium between particulate nitrate and gaseous HNO_3. During the study period, not only the average concentration of NO_2 is higher among PD, but also there is significate difference between PD and CD NOR. The average values of NOR are 0.32 in PD, 0.25 in CD respectively which manifests that the more secondary transformation and pollution potential in PD. On the contrast, the SOR stays constant at high value (~ 0.5) during the whole RH scale which shows different pattern with previously research (Li et al., 2017; Zheng et al., 2015). One possible explanation is that SO_2 concentration stays low level during the whole campaign (4.4 ± 2.4 ppbv on average) and SO_2 oxidation depends on limit of SO_2 instead of oxidation capability. Meanwhile, mean SOR in both situations are over 0.5 (0.52 in CD and 0.56 in PD), further supporting the SO_2 limited hypothesis. Besides, Table 2 summaries NOR and SOR values in YRD. NOR and SOR in this study are similar with values reported in other YRD research (Shu et al., 2019; Zhang et al., 2020b; Qin et al., 2021; Zhao et al., 2022), except values in 2013 (Wang et al., 2016),

https://doi.org/10.5194/acp-2022-548
Preprint. Discussion started: 12 August 2022

Atmospheric Chemistry and Physics Discussions

but higher than north China study (Cao et al., 2017) which emphasize the strong atmospheric oxidation capacity in YRD region.

Table 2 Statistical result of NOR and SOR in YRD

Location and Year	SOR				NOR				References
	Max	Min	Mean	SD	Max	Min	Mean	SD	
Nanjing 2013 Winter	0.42	0.10	0.28	0.11	0.29	0.15	0.21	0.05	
Suzhou 2013 Winter	0.41	0.15	0.27	0.11	0.30	0.06	0.16	0.08	
Lin'an 2013 Winter	0.50	0.19	0.35	0.11	0.24	0.12	0.18	0.05	(Wang et al., 2016)
Hanghou 2013 Winter	0.30	0.14	0.21	0.06	0.11	0.06	0.09	0.02	
Ningbo 2013 Winter	0.35	0.09	0.21	0.11	0.23	0.03	0.11	0.07	
YRD 2016 Summer	-	-	0.347	-	-	-	0.11	-	(Shu et al., 2019)
YRD 2016 Winter	-	-	0.247	-	-	-	0.15	-	
Nanjing 2019 spring	0.48	0.38	-	-	0.31	0.29	-	-	(Qin et al., 2021)
Changzhou 2019 spring	0.35	0.3	-	-	0.27	0.23	-	-	
Changzhou 2019 Winter	0. 68	0.24	0.35	0.12	0.44	0.13	0.2	0.1	(Zhang et al., 2020b)
Changzhou 2019 Summer	0.16	0.76	0.54	0.1	0.08	0.63	0.28	0.14	This work

3.3 The derivation of N_2O_5 uptake coefficient

Statistical analysis of observation above highlights the fast formation of particulate nitrate. In order to assess the contribution of N_2O_5 hydrolysis to particular nitrate formation, two methods are applied to calculate N_2O_5 uptake coefficient. The first method is stationary-state approximation (Brown et al., 2003). By assuming that the rates of production and loss of N_2O_5 are approximately in balance, the total loss rate of N_2O_5 ($k_{N_2O_5}$) can be calculated through equation 9. The $k_{N_2O_5}$ is main dominated by N_2O_5 heterogeneous uptake, since homogeneous hydrolysis of N_2O_5 contributes very little (Brown and Stutz, 2012). N_2O_5 uptake coefficient through steady-state (note as $\gamma_{\_S}$) is derived as equation 10. Here C is the mean molecule speed of N_2O_5, S_a is the aerosol surface concentration.

$$\tau_{ss}(N_2O_5) = \frac{[N_2O_5]}{k_{R3.1}[NO_2][O_3]} = \left(k_{N_2O_5} + \frac{k_{NO_3}}{K_{eq}[NO_2]}\right)^{-1} \quad \text{Eq9}$$

$$k_{N_2O_5} = 0.25\, C\, \gamma_{\_S}\, S_a \quad \text{Eq10}$$

Due to fast variety of NO_3 loss rate from VOCs, the steady-state method has been

https://doi.org/10.5194/acp-2022-548
Preprint. Discussion started: 12 August 2022

Atmospheric Chemistry and Physics Discussions

unattainable in conditions affected by emission interferences. During the whole campaign, we only retrieve three valid fitting results. As shown in Figure 5, the fitted γ_S are ranged from 0.057 to 0.123, which are comparable with Taizhou (0.041, Wang et al. (2020a)) and much higher than other results in China (Yu et al., 2020a; Wang et al., 2018a; Wang et al., 2020b; Wang et al., 2017a). The calculated k_{NO_3} ranged from 0.002 to 0.16 s^{-1}, represents drastic VOCs change during this campaign.

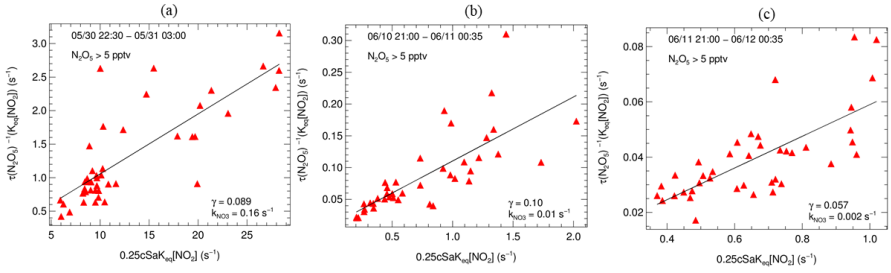

Figure 5 Derived N_2O_5 uptake coefficients from N_2O_5 steady lifetime ($\gamma(N_2O_5\_S)$) with NO_2 and S_a, plots (a-c) represent the linear fitting results at the nights of 05/30, 06/10 and 06/11, respectively.

The other approach is the parameterization by (Yu et al., 2020a) which depicted as follows:

$$\gamma_P = \frac{4}{c}\frac{V_a}{S_a} K_H \times 3.0 \times 10^4 \times [H_2O] \left(1 - \frac{1}{\left(0.033 \times \frac{[H_2O]}{[NO_3^-]}\right) + 1 + \left(3.4 \times \frac{[Cl^-]}{[NO_3^-]}\right)}\right) \quad \text{Eq11}$$

where V_a/S_a is the measured aerosol volume to surface area ratio by SMPS; K_H is Henry's law coefficient which is set as 51 as recommended; $[NO_3^-]$ and $[Cl^-]$ are aerosol inorganic concentration measured by Marga; $[H_2O]$ is aerosol water content calculated through ISORROPIA II. The parameterization calculated N_2O_5 uptake coefficient (note as γ_P) vary from 0.014 to 0.094 with average 0.035.

Furthermore, we compare the difference between γ_S and γ_P. Taking the night of May 30th as example, the γ_S is 0.10 while γ_P ranges from 0.021 to 0.037 with average value as 0.026. The difference between steady-state and parameterization is significant.

https://doi.org/10.5194/acp-2022-548
Preprint. Discussion started: 12 August 2022

Atmospheric Chemistry and Physics Discussions

3.4 Quantifying the contribution of nitrate formation pathways

After the N_2O_5 uptake coefficient counted, nitrate production potential ($P(NO_3^-)$) can be calculated. Here N_2O_5 uptake coefficient is set as 0.035 which is the average value derived from parameterization, while the production ratio of NO_3^- (by considering $ClNO_2$ yield of 0.54) is set as 1.46 from former study (Xia et al., 2020). Gas particle distribution is considered by the result of particular nitrate and gas-phase nitrate by MARGA (input HNO_3/NO_3^- ratio to the model as OH + NO_2 nitrate production rate). Subsequent discussion focuses on OH + NO_2 and N_2O_5 heterogeneous uptake.

The mean diurnal variations of nitrate production potential of clean and polluted day are depicted in Figure 6. The OH + NO_2 pathway shows no significate difference between clean and polluted day and dominate clean day nitrate formation potential. Since the level of OH and NO_2 less affected by the fine particle level. However, the rapid increase of N_2O_5 heterogeneous uptake pathway on polluted day is fatal and its peak formation rate at night over OH + NO_2 pathway which can be used to explain nighttime nitrate explosive growth.

As shown as Figure 6c, OH + NO_2 dominate nitrate production on clean day, while N_2O_5 uptake pathway only contributes 13.2 μg m^{-3}. On polluted days, the ability of N_2O_5 uptake grow fast which reached 25.3 μg m^{-3}, while OH pathway don't change too much. There is no distinct difference of daytime pathway (OH + NO_2) between clean day and polluted day, while nighttime pathway ratio rises from 38.4 % on clean day to 52.9 % on polluted day. The contribution of N_2O_5 hydrolysis on particular nitrate is vital at pollution condition.

https://doi.org/10.5194/acp-2022-548
Preprint. Discussion started: 12 August 2022

Atmospheric Chemistry and Physics Discussions

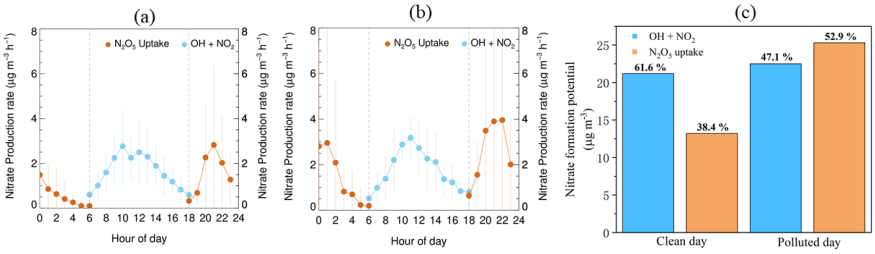

Figure 6 The mean diurnal variations of nitrate production potential of clean day(a) and polluted day (b) and the P(NO_3^-) distribution of clean and polluted day (c).

3.5 Mitigation strategies of particulate nitrate and ozone productions

We selected two pollution episodes (Episode I (2019.05.30 00:00 - 2019.06.02 00:00) and IV (2019.06.14 17:30 - 2019.06.17 12:00)) to explore the mitigation way of ozone and nitrate pollution. Figure 7 shows the EKMA of P(O_3) and P(NO_3^-) of these two periods, O_3 located at VOCs controlling area in the two pollution episodes which consist with previous YRD urban ozone sensitivity study (Jiang et al., 2018; Zhang et al., 2020a; Xu et al., 2021). The best precursor reduction for O_3 is VOCs: NO_x = 2:1 while nitrate located at transition area which means either of precursors reduction will mitigate nitrate pollution. For the regional and complex air pollution characteristics in this region, a fine particle-targeting reduction scheme will aggravate O_3 pollution. In contrast, the O_3-targeting scheme can mitigate O_3 and fine particle simultaneously.

https://doi.org/10.5194/acp-2022-548
Preprint. Discussion started: 12 August 2022

Atmospheric Chemistry and Physics Discussions

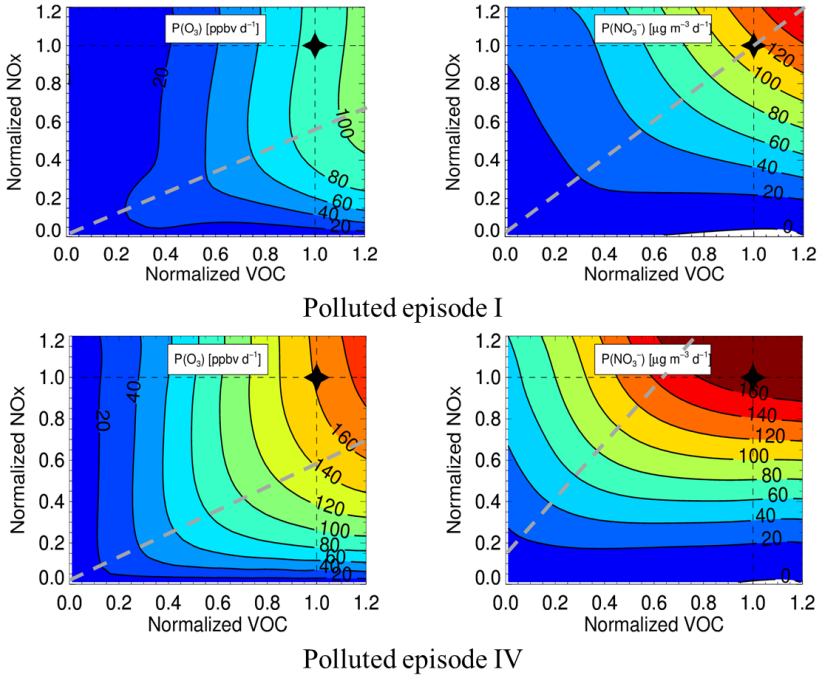

Figure 7 Isogram of $P(O_3)$ and $P(NO_3^-)$ of polluted episode I (2019.05.30 00:00 - 2019.06.02 00:00) and IV (2019.06.14 17:30 - 2019.06.17 12:00) with different NOx and VOC reduction degree. Grey dash line represents the ridge line.

4 Conclusion

A comprehensive campaign was conducted to interpret the atmospheric oxidation capacity and aerosol formation during May 30th to June 18th 2019 at Changzhou, China. The high O_3 and $PM_{2.5}$ concentration confirm complex air pollution characteristics in Changzhou and nitrate accounts for 38.3 % mass concentration of water-soluble components and 32.0 % total $PM_{2.5}$. In addition, the average values of NOR are 0.32 in PD, 0.25 in CD. The positive correlation between NOR and RH and inverse correlation refer the contribution of N_2O_5 heterogenous uptake to nitrate formation.

Based on field observations of OH and related parameters, we show OH oxidation of NO_2 pathway steadily contribute to nitrate formation no matter clean or polluted period and domination clean day nitrate production (about 22 μg m^{-3}). N_2O_5

https://doi.org/10.5194/acp-2022-548
Preprint. Discussion started: 12 August 2022

Atmospheric Chemistry and Physics Discussions

heterogeneous uptake contribution grow rapidly on polluted day, from 13.2 μg m^{-3} (38.4 %) in clean days to 25.3 μg m^{-3} (52.9 %) in polluted days.

The precursor reduction simulation suggests the reduction ratio of VOCs:NO_x equals 2:1 can simultaneously and effectively mitigate O_3 and fine particle pollution during summertime complex pollution period in Changzhou. In order to more precisely and delicately establish cooperative control scheme for regional O_3 and nitrate, the regional and long-time filed campaigns are needed in the future, to analyze seasonal and interannual variation of O_3 and nitrate and relevant parameters.

Code/Data availability. The datasets used in this study are available from the corresponding author upon request (k.lu@pku.edu.cn).

Author contributions. K.D.L. and Y.H.Z. designed the study. T.Y.Z analyzed the data and wrote the paper with input from all authors.

Competing interests. The authors declare that they have no conflicts of interest.

Acknowledgments. This project is supported by the National Natural Science Foundation of China (21976006); the Beijing Municipal Natural Science Foundation for Distinguished Young Scholars (JQ19031); the National Research Program for Key Issue in Air Pollution Control (DQGG0103-01, 2019YFC0214800). Thanks for the data contributed by field campaign team.

References

Andreae, M. O., Schmid, O., Yang, H., Chand, D., Yu, J. Z., Zeng, L.-M., and Zhang, Y.-H.: Optical properties and chemical composition of the atmospheric aerosol in urban Guangzhou, China, Atmos. Environ., 42, 6335-6350, 10.1016/j.atmosenv.2008.01.030, 2008.

Bertram, T. H. and Thornton, J. A.: Toward a general parameterization of N2O5 reactivity on aqueous particles: the competing effects of particle liquid water, nitrate and chloride, Atmospheric Chemistry and Physics, 9, 8351-8363, 10.5194/acp-9-8351-2009, 2009.

Bohn, B., Corlett, G. K., Gillmann, M., Sanghavi, S., Stange, G., Tensing, E., Vrekoussis, M., Bloss, W. J., Clapp, L. J., Kortner, M., Dorn, H. P., Monks, P. S., Platt, U., Plass-Dülmer, C., Mihalopoulos, N., Heard, D. E., Clemitshaw, K. C.,

https://doi.org/10.5194/acp-2022-548
Preprint. Discussion started: 12 August 2022


Atmospheric Chemistry and Physics Discussions

414 Meixner, F. X., Prevot, A. S. H., and Schmitt, R.: Photolysis frequency measurement
415 techniques: results of a comparison within the ACCENT project, ACP, 8, 5373-5391,
416 10.5194/acp-8-5373-2008, 2008.
417 Brown, S. S. and Stutz, J.: Nighttime radical observations and chemistry, Chemical
418 Society Reviews, 41, 6405-6447, 10.1039/c2cs35181a, 2012.
419 Brown, S. S., Stark, H., and Ravishankara, A. R.: Applicability of the steady state
420 approximation to the interpretation of atmospheric observations of NO3 and N2O5,
421 Journal of Geophysical Research-Atmospheres, 108, 10, 10.1029/2003jd003407,
422 2003.
423 Brown, S. S., Dube, W. P., Fuchs, H., Ryerson, T. B., Wollny, A. G., Brock, C. A.,
424 Bahreini, R., Middlebrook, A. M., Neuman, J. A., Atlas, E., Roberts, J. M., Osthoff,
425 H. D., Trainer, M., Fehsenfeld, F. C., and Ravishankara, A. R.: Reactive uptake
426 coefficients for N2O5 determined from aircraft measurements during the Second
427 Texas Air Quality Study: Comparison to current model parameterizations, Journal of
428 Geophysical Research-Atmospheres, 114, 10.1029/2008jd011679, 2009.
429 Burkholder, J. B., Sander, S. P., Abbatt, J., Barker, J., Huie, R., Kolb, C. E., Kurylo,
430 M., Orkin, V., Wilmouth, D. M., and Wine, P.: Chemical Kinetics and Photochemical
431 Data for Use in Atmospheric Studies, Evaluation Number 18,
432 10.13140/RG.2.1.2504.2806, 2015.
433 Cao, J.-J., Shen, Z.-X., Chow, J. C., Watson, J. G., Lee, S.-C., Tie, X.-X., Ho, K.-F.,
434 Wang, G.-H., and Han, Y.-M.: Winter and Summer PM2.5 Chemical Compositions in
435 Fourteen Chinese Cities, Journal of the Air & Waste Management Association, 62,
436 1214-1226, 10.1080/10962247.2012.701193, 2012.
437 Cao, Z., Zhou, X., Ma, Y., Wang, L., Wu, R., Chen, B., and Wang, W.: The
438 Concentrations, Formations, Relationships and Modeling of Sulfate, Nitrate and
439 Ammonium (SNA) Aerosols over China, Aerosol and Air Quality Research, 17, 84-
440 97, 10.4209/aaqr.2016.01.0020, 2017.
441 Chang, Y. H., Zhang, Y. L., Tian, C. G., Zhang, S. C., Ma, X. Y., Cao, F., Liu, X. Y.,
442 Zhang, W. Q., Kuhn, T., and Lehmann, M. F.: Nitrogen isotope fractionation during
443 gas-to-particle conversion of NOx to NO3- in the atmosphere - implications for
444 isotope-based NOx source apportionment, Atmospheric Chemistry and Physics, 18,
445 11647-11661, 10.5194/acp-18-11647-2018, 2018.
446 Chen, H., Hu, R., Xie, P., Xing, X., Ling, L., Li, Z., Wang, F., Wang, Y., Liu, J., and
447 Liu, W.: A hydroxyl radical detection system using gas expansion and fast gating
448 laser-induced fluorescence techniques, J. Environ. Sci., 65, 190-200,
449 10.1016/j.jes.2017.03.012, 2018.
450 Chen, X., Walker, J. T., and Geron, C.: Chromatography related performance of the
451 Monitor for AeRosols and GAses in ambient air (MARGA): laboratory and field-
452 based evaluation, Atmos. Meas. Tech., 10, 3893-3908, 10.5194/amt-10-3893-2017,
453 2017.
454 Chen, X. R., Wang, H. C., Liu, Y. H., Su, R., Wang, H. L., Lou, S. R., and Lu, K. D.:
455 Spatial characteristics of the nighttime oxidation capacity in the Yangtze River Delta,

https://doi.org/10.5194/acp-2022-548
Preprint. Discussion started: 12 August 2022


Atmospheric Chemistry and Physics Discussions

China, Atmospheric Environment, 208, 150-157, 10.1016/j.atmosenv.2019.04.012, 2019.
Chen, X. R., Wang, H. C., Lu, K. D., Li, C. M., Zhai, T. Y., Tan, Z. F., Ma, X. F., Yang, X. P., Liu, Y. H., Chen, S. Y., Dong, H. B., Li, X., Wu, Z. J., Hu, M., Zeng, L. M., and Zhang, Y. H.: Field Determination of Nitrate Formation Pathway in Winter Beijing, Environmental Science & Technology, 54, 9243-9253, 10.1021/acs.est.0c00972, 2020.
Elshorbany, Y. F., Steil, B., Brühl, C., and Lelieveld, J.: Impact of HONO on global atmospheric chemistry calculated with an empirical parameterization in the EMAC model, ACP, 12, 9977-10000, 10.5194/acp-12-9977-2012, 2012.
Fountoukis, C. and Nenes, A.: ISORROPIA II: a computationally efficient thermodynamic equilibrium model for K+-Ca2+-Mg2+-Nh(4)(+)-Na+-SO42--NO3--Cl--H2O aerosols, Atmospheric Chemistry and Physics, 7, 4639-4659, 2007.
Goliff, W. S., Stockwell, W. R., and Lawson, C. V.: The regional atmospheric chemistry mechanism, version 2, Atmospheric Environment, 68, 174-185, 10.1016/j.atmosenv.2012.11.038, 2013.
Guo, L., Hu, Y., Hu, Q., Lin, J., Li, C., Chen, J., Li, L., and Fu, H.: Characteristics and chemical compositions of particulate matter collected at the selected metro stations of Shanghai, China, Science of the Total Environment, 496, 443-452, 10.1016/j.scitotenv.2014.07.055, 2014.
Hagler, G. S. W., Bergin, M. H., Salmon, L. G., Yu, J. Z., Wan, E. C. H., Zheng, M., Zeng, L. M., Kiang, C. S., Zhang, Y. H., Lau, A. K. H., and Schauer, J. J.: Source areas and chemical composition of fine particulate matter in the Pearl River Delta region of China, Atmos. Environ., 40, 3802-3815, 10.1016/j.atmosenv.2006.02.032, 2006.
Jiang, M., Lu, K., Su, R., Tan, Z., Wang, H., Li, L., Fu, Q., Zhai, C., Tan, Q., Yue, D., Chen, D., Wang, Z., Xie, S., Zeng, L., and Zhang, Y.: Ozone formation and key VOCs in typical Chinese city clusters, Chinese Sci Bull, 63, 1130-1141, 2018.
Kanaya, Y., Fukuda, M., Akimoto, H., Takegawa, N., Komazaki, Y., Yokouchi, Y., Koike, M., and Kondo, Y.: Urban photochemistry in central Tokyo: 2. Rates and regimes of oxidant (O-3+NO2) production, Journal of Geophysical Research-Atmospheres, 113, 10.1029/2007jd008671, 2008.
Li, H. Y., Zhang, Q., Zhang, Q., Chen, C. R., Wang, L. T., Wei, Z., Zhou, S., Parworth, C., Zheng, B., Canonaco, F., Prevot, A. S. H., Chen, P., Zhang, H. L., Wallington, T. J., and He, K. B.: Wintertime aerosol chemistry and haze evolution in an extremely polluted city of the North China Plain: significant contribution from coal and biomass combustion, Atmospheric Chemistry and Physics, 17, 4751-4768, 10.5194/acp-17-4751-2017, 2017.
Liu, X., Gu, J., Li, Y., Cheng, Y., Qu, Y., Han, T., Wang, J., Tian, H., Chen, J., and Zhang, Y.: Increase of aerosol scattering by hygroscopic growth: Observation, modeling, and implications on visibility, Atmos. Res., 132-133, 91-101, https://doi.org/10.1016/j.atmosres.2013.04.007, 2013.

https://doi.org/10.5194/acp-2022-548
Preprint. Discussion started: 12 August 2022

498 Lou, S., Tan, Z., Gan, G., Chen, J., Wang, H., Gao, Y., Huang, D., Huang, C., Li, X.,
499 Song, R., Wang, H., Wang, M., Wang, Q., Wu, Y., and Huang, C.: Observation based
500 study on atmospheric oxidation capacity in Shanghai during late-autumn:
501 Contribution from nitryl chloride, Atmospheric Environment, 271, 118902,
502 https://doi.org/10.1016/j.atmosenv.2021.118902, 2022.
503 Lu, K. D., Hofzumahaus, A., Holland, F., Bohn, B., Brauers, T., Fuchs, H., Hu, M.,
504 Haseler, R., Kita, K., Kondo, Y., Li, X., Lou, S. R., Oebel, A., Shao, M., Zeng, L. M.,
505 Wahner, A., Zhu, T., Zhang, Y. H., and Rohrer, F.: Missing OH source in a suburban
506 environment near Beijing: observed and modelled OH and HO2 concentrations in
507 summer 2006, Atmospheric Chemistry and Physics, 13, 1057-1080, 10.5194/acp-13-
508 1057-2013, 2013.
509 Lu, K. D., Rohrer, F., Holland, F., Fuchs, H., Bohn, B., Brauers, T., Chang, C. C.,
510 Haseler, R., Hu, M., Kita, K., Kondo, Y., Li, X., Lou, S. R., Nehr, S., Shao, M., Zeng,
511 L. M., Wahner, A., Zhang, Y. H., and Hofzumahaus, A.: Observation and modelling
512 of OH and HO2 concentrations in the Pearl River Delta 2006: a missing OH source in
513 a VOC rich atmosphere, Atmospheric Chemistry and Physics, 12, 1541-1569,
514 10.5194/acp-12-1541-2012, 2012.
515 Ma, X. F., Tan, Z. F., Lu, K. D., Yang, X. P., Chen, X. R., Wang, H. C., Chen, S. Y.,
516 Fang, X., Li, S. L., Li, X., Liu, J. W., Liu, Y., Lou, S. R., Qiu, W. Y., Wang, H. L.,
517 Zeng, L. M., and Zhang, Y. H.: OH and HO2 radical chemistry at a suburban site
518 during the EXPLORE-YRD campaign in 2018, Atmospheric Chemistry and Physics,
519 22, 7005-7028, 2022.
520 Meng, Z. Y., Wu, L. Y., Xu, X. D., Xu, W. Y., Zhang, R. J., Jia, X. F., Liang, L. L.,
521 Miao, Y. C., Cheng, H. B., Xie, Y. L., He, J. J., and Zhong, J. T.: Changes in
522 ammonia and its effects on PM2.5 chemical property in three winter seasons in
523 Beijing, China, Science of the Total Environment, 749, 2020.
524 Ming, L., Jin, L., Li, J., Fu, P., Yang, W., Liu, D., Zhang, G., Wang, Z., and Li, X.:
525 PM2.5 in the Yangtze River Delta, China: Chemical compositions, seasonal
526 variations, and regional pollution events, Environmental Pollution, 223, 200-212,
527 10.1016/j.envpol.2017.01.013, 2017.
528 Phillips, G. J., Thieser, J., Tang, M. J., Sobanski, N., Schuster, G., Fachinger, J.,
529 Drewnick, F., Borrmann, S., Bingemer, H., Lelieveld, J., and Crowley, J. N.:
530 Estimating N2O5 uptake coefficients using ambient measurements of NO3, N2O5,
531 ClNO2 and particle-phase nitrate, Atmospheric Chemistry and Physics, 16, 13231-
532 13249, 10.5194/acp-16-13231-2016, 2016.
533 Qin, Y., Li, J. Y., Gong, K. J., Wu, Z. J., Chen, M. D., Qin, M. M., Huang, L., and
534 Hu, J. L.: Double high pollution events in the Yangtze River Delta from 2015 to 2019:
535 Characteristics, trends, and meteorological situations, Science of the Total
536 Environment, 792, 10.1016/j.scitotenv.2021.148349, 2021.
537 Seinfeld, J. H. and Pandis, S. N.: Atmospheric chemistry and physics: from air
538 pollution to climate change, Third;3rd;, Book, Whole, Wiley, Hoboken, New
539 Jersey2016.

https://doi.org/10.5194/acp-2022-548
Preprint. Discussion started: 12 August 2022


Atmospheric Chemistry and Physics Discussions

Shang, D. J., Peng, J. F., Guo, S., Wu, Z. J., and Hu, M.: Secondary aerosol formation in winter haze over the Beijing-Tianjin-Hebei Region, China, Front. Env. Sci. Eng., 15, 13, 10.1007/s11783-020-1326-x, 2021.

Shu, L., Wang, T. J., Xie, M., Li, M. M., Zhao, M., Zhang, M., and Zhao, X. Y.: Episode study of fine particle and ozone during the CAPUM-YRD over Yangtze River Delta of China: Characteristics and source attribution, Atmos. Environ., 203, 87-101, 10.1016/j.atmosenv.2019.01.044, 2019.

Song, C. H. and Carmichael, G. R.: Gas-particle partitioning of nitric acid modulated by alkaline aerosol, Journal of Atmospheric Chemistry, 40, 1-22, 2001.

Staudt, S., Gord, J. R., Karimova, N. V., McDuffie, E. E., Brown, S. S., Gerber, R. B., Nathanson, G. M., and Bertram, T. H.: Sulfate and Carboxylate Suppress the Formation of ClNO2 at Atmospheric Interfaces, Acs Earth and Space Chemistry, 3, 1987-1997, 2019.

Sun, Y. L., Zhuang, G. S., Tang, A. H., Wang, Y., and An, Z. S.: Chemical characteristics of PM2.5 and PM10 in haze-fog episodes in Beijing, Environmental Science & Technology, 40, 3148-3155, 10.1021/es051533g, 2006.

Tan, Z., Wang, H., Lu, K., Dong, H., Liu, Y., Zeng, L., Hu, M., and Zhang, Y.: An Observational Based Modeling of the Surface Layer Particulate Nitrate in the North China Plain During Summertime, Journal of Geophysical Research: Atmospheres, 126, e2021JD035623, https://doi.org/10.1029/2021JD035623, 2021.

Tan, Z. F., Lu, K. D., Dong, H. B., Hu, M., Li, X., Liu, Y. H., Lu, S. H., Shao, M., Su, R., Wang, H. C., Wu, Y. S., Wahner, A., and Zhang, Y. H.: Explicit diagnosis of the local ozone production rate and the ozone-NOx-VOC sensitivities, Science Bulletin, 63, 1067-1076, 10.1016/j.scib.2018.07.001, 2018.

Tan, Z. F., Fuchs, H., Lu, K. D., Hofzumahaus, A., Bohn, B., Broch, S., Dong, H. B., Gomm, S., Haseler, R., He, L. Y., Holland, F., Li, X., Liu, Y., Lu, S. H., Rohrer, F., Shao, M., Wang, B. L., Wang, M., Wu, Y. S., Zeng, L. M., Zhang, Y. S., Wahner, A., and Zhang, Y. H.: Radical chemistry at a rural site (Wangdu) in the North China Plain: observation and model calculations of OH, HO2 and RO2 radicals, Atmospheric Chemistry and Physics, 17, 663-690, 10.5194/acp-17-663-2017, 2017.

Tham, Y. J., Wang, Z., Li, Q., Wang, W., Wang, X., Lu, K., Ma, N., Yan, C., Kecorius, S., Wiedensohler, A., Zhang, Y., and Wang, T.: Heterogeneous N2O5 uptake coefficient and production yield of ClNO2 in polluted northern China: roles of aerosol water content and chemical composition, Atmospheric Chemistry and Physics, 18, 13155-13171, 10.5194/acp-18-13155-2018, 2018.

Wang, H., Zhu, B., Shen, L., Xu, H., An, J., Pan, C., Li, Y. e., and Liu, D.: Regional Characteristics of Air Pollutants during Heavy Haze Events in the Yangtze River Delta, China, Aerosol and Air Quality Research, 16, 2159-2171, 10.4209/aaqr.2015.09.0551, 2016.

Wang, H., Lu, K., Chen, X., Zhu, Q., Chen, Q., Guo, S., Jiang, M., Li, X., Shang, D., Tan, Z., Wu, Y., Wu, Z., Zou, Q., Zheng, Y., Zeng, L., Zhu, T., Hu, M., and Zhang, Y.: High N2O5 Concentrations Observed in Urban Beijing: Implications of a Large

https://doi.org/10.5194/acp-2022-548
Preprint. Discussion started: 12 August 2022


Atmospheric Chemistry and Physics Discussions

582 Nitrate Formation Pathway, Environmental Science and Technology Letters, 4, 416-
583 420, 10.1021/acs.estlett.7b00341, 2017a.
584 Wang, H. C. and Lu, K. D.: Determination and Parameterization of the Heterogeneous
585 Uptake Coefficient of Dinitrogen Pentoxide (N2O5), Prog. Chem., 28, 917-933,
586 10.7536/pc151225, 2016.
587 Wang, H. C., Chen, J., and Lu, K. D.: Development of a portable cavity-enhanced
588 absorption spectrometer for the measurement of ambient NO3 and N2O5:
589 experimental setup, lab characterizations, and field applications in a polluted urban
590 environment, Atmos. Meas. Tech., 10, 1465-1479, 10.5194/amt-10-1465-2017,
591 2017b.
592 Wang, H. C., Lu, K. D., Chen, X. R., Zhu, Q. D., Wu, Z. J., Wu, Y. S., and Sun, K.:
593 Fast particulate nitrate formation via N2O5 uptake aloft in winter in Beijing,
594 Atmospheric Chemistry and Physics, 18, 10483-10495, 10.5194/acp-18-10483-2018,
595 2018a.
596 Wang, H. C., Chen, X. R., Lu, K. D., Hu, R. Z., Li, Z. Y., Wang, H. L., Ma, X. F.,
597 Yang, X. P., Chen, S. Y., Dong, H. B., Liu, Y., Fang, X., Zeng, L. M., Hu, M., and
598 Zhang, Y. H.: NO3 and N2O5 chemistry at a suburban site during the EXPLORE-
599 YRD campaign in 2018, Atmospheric Environment, 224, 9,
600 10.1016/j.atmosenv.2019.117180, 2020a.
601 Wang, H. C., Chen, X. R., Lu, K. D., Tan, Z. F., Ma, X. F., Wu, Z. J., Li, X., Liu, Y.
602 H., Shang, D. J., Wu, Y. S., Zeng, L. M., Hu, M., Schmitt, S., Kiendler-Scharr, A.,
603 Wahner, A., and Zhang, Y. H.: Wintertime N2O5 uptake coefficients over the North
604 China Plain, Science Bulletin, 65, 765-774, 10.1016/j.scib.2020.02.006, 2020b.
605 Wang, H. C., Lu, K. D., Guo, S., Wu, Z. J., Shang, D. J., Tan, Z. F., Wang, Y. J., Le
606 Breton, M., Lou, S. R., Tang, M. J., Wu, Y. S., Zhu, W. F., Zheng, J., Zeng, L. M.,
607 Hallquist, M., Hu, M., and Zhang, Y. H.: Efficient N2O5 uptake and NO3 oxidation
608 in the outflow of urban Beijing, Atmospheric Chemistry and Physics, 18, 9705-9721,
609 10.5194/acp-18-9705-2018, 2018b.
610 Wang, S. B., Wang, L. L., Fan, X. G., Wang, N., Ma, S. L., and Zhang, R. Q.:
611 Formation pathway of secondary inorganic aerosol and its influencing factors in
612 Northern China: Comparison between urban and rural sites, Science of the Total
613 Environment, 840, 2022.
614 Wang, X. F., Zhang, Y. P., Chen, H., Yang, X., Chen, J. M., and Geng, F. H.:
615 Particulate Nitrate Formation in a Highly Polluted Urban Area: A Case Study by
616 Single-Particle Mass Spectrometry in Shanghai, Environmental Science &
617 Technology, 43, 3061-3066, 2009.
618 Wang, Z., Wang, W. H., Tham, Y. J., Li, Q. Y., Wang, H., Wen, L., Wang, X. F., and
619 Wang, T.: Fast heterogeneous N2O5 uptake and ClNO2 production in power plant
620 and industrial plumes observed in the nocturnal residual layer over the North China
621 Plain, Atmospheric Chemistry and Physics, 17, 12361-12378, 10.5194/acp-17-12361-
622 2017, 2017c.
623 Woodward-Massey, R., Slater, E. J., Alen, J., Ingham, T., Cryer, D. R., Stimpson, L.

https://doi.org/10.5194/acp-2022-548
Preprint. Discussion started: 12 August 2022


Atmospheric Chemistry and Physics Discussions

624 M., Ye, C. X., Seakins, P. W., Whalley, L. K., and Heard, D. E.: Implementation of a
625 chemical background method for atmospheric OH measurements by laser-induced
626 fluorescence: characterisation and observations from the UK and China, Atmos.
627 Meas. Tech., 13, 3119-3146, 10.5194/amt-13-3119-2020, 2020.
628 Wu, S. P., Dai, L. H., Zhu, H., Zhang, N., Yan, J. P., Schwab, J. J., and Yuan, C. S.:
629 The impact of sea-salt aerosols on particulate inorganic nitrogen deposition in the
630 western Taiwan Strait region, China, Atmos. Res., 228, 68-76, 2019.
631 Xia, M., Peng, X., Wang, W., Yu, C., Sun, P., Li, Y., Liu, Y., Xu, Z., Wang, Z., Xu,
632 Z., Nie, W., Ding, A., and Wang, T.: Significant production of ClNO2 and possible
633 source of Cl-2 from N2O5 uptake at a suburban site in eastern China, Atmospheric
634 Chemistry and Physics, 20, 6147-6158, 10.5194/acp-20-6147-2020, 2020.
635 Xu, J. W., Huang, X., Wang, N., Li, Y. Y., and Ding, A. J.: Understanding ozone
636 pollution in the Yangtze River Delta of eastern China from the perspective of diurnal
637 cycles, Science of the Total Environment, 752, 10.1016/j.scitotenv.2020.141928,
638 2021.
639 Xue, H., Liu, G., Zhang, H., Hu, R., and Wang, X.: Similarities and differences in
640 PM10 and PM2.5 concentrations, chemical compositions and sources in Hefei City,
641 China, Chemosphere, 220, 760-765, 10.1016/j.chemosphere.2018.12.123, 2019.
642 Yang, X. P., Lu, K. D., Ma, X. F., Liu, Y. H., Wang, H. C., Hu, R. Z., Li, X., Lou, S.
643 R., Chen, S. Y., Dong, H. B., Wang, F. Y., Wang, Y. H., Zhang, G. X., Li, S. L.,
644 Yang, S. D., Yang, Y. M., Kuang, C. L., Tan, Z. F., Chen, X. R., Qiu, P. P., Zeng, L.
645 M., Xie, P. H., and Zhang, Y. H.: Observations and modeling of OH and HO2 radicals
646 in Chengdu, China in summer 2019, Science of the Total Environment, 772, 2021.
647 Yu, C., Wang, Z., Xia, M., Fu, X., Wang, W. H., Tham, Y. J., Chen, T. S., Zheng, P.
648 G., Li, H. Y., Shan, Y., Wang, X. F., Xue, L. K., Zhou, Y., Yue, D. L., Ou, Y. B.,
649 Gao, J., Lu, K. D., Brown, S. S., Zhang, Y. H., and Wang, T.: Heterogeneous N2O5
650 reactions on atmospheric aerosols at four Chinese sites: improving model
651 representation of uptake parameters, Atmospheric Chemistry and Physics, 20, 4367-
652 4378, 10.5194/acp-20-4367-2020, 2020a.
653 Yu, D., Tan, Z., Lu, K., Ma, X., Li, X., Chen, S., Zhu, B., Lin, L., Li, Y., Qiu, P.,
654 Yang, X., Liu, Y., Wang, H., He, L., Huang, X., and Zhang, Y.: An explicit study of
655 local ozone budget and NOx-VOCs sensitivity in Shenzhen China, Atmospheric
656 Environment, 224, 117304, 10.1016/j.atmosenv.2020.117304, 2020b.
657 Zhang, K., Xu, J. L., Huang, Q., Zhou, L., Fu, Q. Y., Duan, Y. S., and Xiu, G. L.:
658 Precursors and potential sources of ground-level ozone in suburban Shanghai, Front.
659 Env. Sci. Eng., 14, 10.1007/s11783-020-1271-8, 2020a.
660 Zhang, R., Han, Y. H., Shi, A. J., Sun, X. S., Yan, X., Huang, Y. H., and Wang, Y.:
661 Characteristics of ambient ammonia and its effects on particulate ammonium in
662 winter of urban Beijing, China, Environ Sci Pollut R, 28, 62828-62838, 2021.
663 Zhang, Y., Hong, Z., Chen, J., Xu, L., Hong, Y., Li, M., Hao, H., Chen, Y., Qiu, Y.,
664 Wu, X., Li, J.-R., Tong, L., and Xiao, H.: Impact of control measures and typhoon
665 weather on characteristics and formation of PM2.5 during the 2016 G20 summit in

https://doi.org/10.5194/acp-2022-548
Preprint. Discussion started: 12 August 2022

Atmospheric Chemistry and Physics Discussions

China, Atmos. Environ., 224, 117312, https://doi.org/10.1016/j.atmosenv.2020.117312, 2020b.

Zhang, Y., Tang, L., Yu, H., Wang, Z., Sun, Y., Qin, W., Chen, W., Chen, C., Ding, A., Wu, J., Ge, S., Chen, C., and Zhou, H.-c.: Chemical composition, sources and evolution processes of aerosol at an urban site in Yangtze River Delta, China during wintertime, Atmospheric Environment, 123, 339-349, 10.1016/j.atmosenv.2015.08.017, 2015.

Zhang, Y., Tang, L., Croteau, P. L., Favez, O., Sun, Y., Canagaratna, M. R., Wang, Z., Couvidat, F., Albinet, A., Zhang, H., Sciare, J., Prevot, A. S. H., Jayne, J. T., and Worsnop, D. R.: Field characterization of the PM2.5 Aerosol Chemical Speciation Monitor: insights into the composition, sources, and processes of fine particles in eastern China, Atmospheric Chemistry and Physics, 17, 14501-14517, 10.5194/acp-17-14501-2017, 2017.

Zhang, Y. Y., Tang, A. H., Wang, C., Ma, X., Li, Y. Z., Xu, W., Xia, X. P., Zheng, A. H., Li, W. Q., Fang, Z. G., Zhao, X. F., Peng, X. L., Zhang, Y. P., Han, J., Zhang, L. J., Collett, J. L., and Liu, X. J.: PM (2.5) and water-soluble inorganic ion concentrations decreased faster in urban than rural areas in China, J. Environ. Sci., 122, 83-91, 2022.

Zhao, P. S., Dong, F., He, D., Zhao, X. J., Zhang, X. L., Zhang, W. Z., Yao, Q., and Liu, H. Y.: Characteristics of concentrations and chemical compositions for PM2.5 in the region of Beijing, Tianjin, and Hebei, China, Atmospheric Chemistry and Physics, 13, 4631-4644, 10.5194/acp-13-4631-2013, 2013.

Zhao, Z. Z., Sun, N., Zhou, W. L., Ma, S. S., Li, X. D., Li, M. L., Zhang, X., Tang, S. S., and Ye, Z. L.: Chemical Compositions in Winter PM2.5 in Changzhou of the Yangtze River Delta Region, China: Characteristics and Atmospheric Responses Along With the Different Pollution Levels, Front Env Sci-Switz, 10, 2022.

Zheng, G. J., Duan, F. K., Su, H., Ma, Y. L., Cheng, Y., Zheng, B., Zhang, Q., Huang, T., Kimoto, T., Chang, D., Poschl, U., Cheng, Y. F., and He, K. B.: Exploring the severe winter haze in Beijing: the impact of synoptic weather, regional transport and heterogeneous reactions, Atmospheric Chemistry and Physics, 15, 2969-2983, 10.5194/acp-15-2969-2015, 2015.